*Journal of The Electrochemical Society*, **163** (7) A1484-A1492 (2016)
0013-4651/2016/163(7)/A1484/9/$33.00 © The Electrochemical Society

# Effect of Electrolyte Additives on $NaTi_2(PO_4)_3$-C//$Na_3V_2O_{2X}(PO_4)_2F_{3-2X}$-MWCNT Aqueous Rechargeable Sodium Ion Battery Performance

**P. Ramesh Kumar,* Young Hwa Jung,*,[a] Brindha Moorthy, and Do Kyung Kim*,[z]**

*Department of Materials Science and Engineering, Korea Advanced Institute of Science and Technology (KAIST), Yuseong-gu, Daejeon 34141, Korea*

Aqueous sodium ion batteries are future low cost and eco-friendly energy storage systems, but aqueous batteries are very much constrained by the electrolyte degradation. In this aspect, we have evaluated effect of salt concentration and electrolyte additives on aqueous sodium ion full cell performance by using $NaTi_2(PO_4)_3$ and $Na_3V_2O_{2X}(PO_4)_2F_{3-2X}$ as anode and cathode materials respectively. Before making full cell, the effect of adding different concentrations of vinylene carbonate (VC), carboxymethyl cellulose (CMC) and agarose (Ag) to aqueous 10 M $NaClO_4$ electrolyte was correlated by using cathode material in half-cell configuration. In full cell, 10 M $NaClO_4$ electrolytes with 2 v% of VC enhances the cycle stability of $NaTi_2(PO_4)_3$-C// $Na_3V_2O_{2X}(PO_4)_2F_{3-2X}$ -MWCNT systems compared to other electrolytes.
 [DOI: 10.1149/2.0031608jes] 

Manuscript submitted March 11, 2016; revised manuscript received April 20, 2016. Published May 12, 2016.

Stationary energy storage systems utilizing electrochemical rechargeable batteries are promising candidates for future power sources for large-scale applications due to long cycle life, controllable power & energy densities in low cost.[1,2] Present, when compared to other conventional rechargeable battery systems, lithium ion batteries show the highest energy density and excellent cycle stability for portable applications. However, in large-scale stationary energy storage applications, the safety, cost, and cycle life become relatively more important than energy density.[3,4] The usage of flammable organic electrolyte causes the thermal runaway by the reactivity of the electrode materials with electrolytes. Hence, current lithium ion batteries fail to meet the above requirements by having organic electrolytes and high processing cost. Presently, one of the behind lithium ion batteries are aqueous rechargeable alkali-metal ion ($Li^+$, $Na^+$) batteries (ARAB's), which are non-flammable, fast ion transportation and lower manufacturing cost, which are most suitable for large scale energy storage applications.[5]

In 1994, Dahn et al. first reported $VO_2$//$LiMn_2O_4$ storage system in lithium aqueous electrolytes. After that, many researchers proposed lithium as well as sodium ion aqueous systems such as $LiV_3O_8$//$LiCoO_2$, $TiP_2O_7$//$LiMn_2O_4$, $LiTi_2(PO_4)_3$//$LiMn_2O_4$, $LiTi_2(PO_4)_3$//$LiFePO_4$, $Na_3Ti_2(PO_4)_3$//$Na_{0.24}MnO_2$, $NaTi_2(PO_4)_3$//$Na_{0.44}MnO_2$, $NaTi_2(PO_4)_3$//$Na_2NiFe(CN)_6$, $NaTi_2(PO_4)_3$//$Na_2CuFe(CN)_6$, Zn//$Na_{0.95}MnO_2$.[6–17] But, still inferior cycle stability has been obtained in the majority of the aqueous rechargeable alkali-metal ion batteries because of side reactions. There are four major side reactions in ARABs while using intercalation electrode, which are greatly influence on their cyclic stability: (a) $H_2$ and $O_2$ evolution (electrolyte decomposition), (b) reactions between electrode materials and $H_2O$ or residual $O_2$ (c) electrode dissolution, and (d) proton co-insertion into the host electrode materials. Researchers have tried to avoid the above-mentioned side reactions by using neutral pH aqueous electrolytes and continuous $N_2$ purging to reduce the effect of residual $O_2$ in aqueous electrolytes. In our recent study, we have reported $NaTi_2(PO_4)_3$//$Na_3V_2O_{2X}(PO_4)_2F_{3-2X}$ system with vinylene carbonate (VC) added 10 M $NaClO_4$ electrolytes, which are having high voltage and stable cycleability.[18] In aqueous electrolyte, vinylene carbonate will isolate the electrodes from reaction with $O_2$ and electrode dissolution by forming a protective layer on electrode surfaces.

In this paper, we address the side reactions like, $H_2$ and $O_2$ evolution, reactions between electrode materials and $H_2O$ or residual $O_2$ and electrode dissolution by using some additives. We studied the effect of vinylene carbonate (VC), carboxymethyl cellulose (CMC) and agarose (Ag) addition on the electrochemical performance of the intercalate compound $Na_3V_2O_{2X}(PO_4)_2F_{3-2X}$-MWCNT in an aqueous 10 M $NaClO_4$ electrolytes. And also, correlate the electrochemical performance of $Na_3V_2O_{2X}(PO_4)_2F_{3-2X}$-MWCNT with respect to the salt, additive concentrations, pH and viscosity. The full cell discharge capacity and energy density of aqueous rechargeable sodium ion batteries [$NaTi_2(PO_4)_3$-C//$Na_3V_2O_{2X}(PO_4)_2F_{3-2X}$-MWCNT] are measured and calculated in the selected aqueous electrolytes. 10 M $NaClO_4$ electrolytes with 2 v% of VC possess enhanced cycle stability of $NaTi_2(PO_4)_3$-C//$Na_3V_2O_{2X}(PO_4)_2F_{3-2X}$-MWCNT systems compared to others. To our best knowledge, this is a first examination of the effect of electrolyte additive on electrochemical properties of aqueous rechargeable sodium ion batteries.

## Experimental

***Synthesis of electrode materials.***—$Na_3V_2O_{2X}(PO_4)_2F_{3-2X}$-MWCNT composite samples were prepared under mild hydrothermal conditions by reacting NaF and $[V(PO_3)_3]_n$-MWCNT in a 3.3:1 molar ratio. The reaction mixture was sealed in a polytetrafluoroethylene (PTFE)-lined steel pressure vessel, which was maintained at 170°C for 72 h. The excess carbon source prevents the complete oxidation from $V^{3+}$ to $V^{4+}$ in an aqueous medium. $[V(PO_3)_3]_n$-MWCNT was synthesized via a solid-state method previously described in literature.[18]

***Preparation of the $NaTi_2(PO_4)_3$-C composite anode.***—Carbon coated $NaTi_2(PO_4)_3$ nanoparticles were prepared by the gel combustion process followed by heat-treatment. The synthesis method to prepare NTP-C was adopted from previously reported work.[19] Initially, titanyl hydroxide [$TiO(OH)_2$] was prepared by hydrolysis of titanium butoxide [$Ti(C_4H_9O)_4$] under ice-cold condition with constant stirring. Then, $HNO_3$ solution was added drop wise to convert the titanyl hydroxide into titanyl nitrate [$Ti(NO_3)_2$]. Then, stoichiometric amount of $NaNO_3$ and $NH_4H_2PO_4$ were added into above solution and the reaction temperature was maintained at 80°C, after dissolution of all added salts, glycine was added, which is used as carbon source to achieve the mole ratio of glycine: nitrate of 2:1. The gelled precursor was obtained after drying of above homogenized solution at 80°C. Then, the auto combustion of gelled precursor was carried out at 200°C in air atmosphere. The fluffy combustion product was formed, further it was heated up to 750°C for 10 h under argon atmosphere to obtain pure crystalline carbon coated $NaTi_2(PO_4)_3$ nanoparticles.

***Characterization.***—The final phase of the $Na_3V_2O_{2x}(PO_4)_2F_{3-2x}$-MWCNT composite was confirmed by synchrotron radiation powder X-ray diffraction (SPXRD) data collected at room temperature from the 9B HRPD beamline of the Pohang Accelerator Laboratory

*Electrochemical Society Member.
[a]Present address: Beamline Department, Pohang Accelerator Laboratory (PAL), Pohang 37673, Korea.
[z]E-mail: dkkim@kaist.ac.kr

(PAL) in Korea at a wavelength of $\lambda = 1.4640$ Å. The diffraction patterns were acquired over an angular range of $10^\circ \leq 2\theta \leq 130^\circ$ at a step width of $0.01^\circ$ using a six multi-detector system. The phase of the $NaTi_2(PO_4)_3$-C composite was confirmed X-ray diffractometer (Rigaku D/Max-2500) with a Cu X-ray ($\lambda = 1.5418$ Å) at room temperature. The particle size and morphology were characterized using a field emission scanning electron microscope (FE-SEM Hitachi S-4800, Japan). The Raman spectra of the powders were recorded at room temperature on a HR 800 Raman spectrophotometer (Jobin Yvon- Horiba, France) using monochromatic a He-Ne laser (514 nm) operating at 20 mW. Elemental analysis (EA) was carried out using a Thermo Scientific Flash 2000 Series element analyzer. XPS measurement was carried with a thermo scientific XPS, sigma probe with energy resolution of 0.46 eV.

***Electrochemical testing.***—The electrochemical studies of the as-synthesized $Na_3V_2O_{2X}(PO_4)_2F_{3-2X}$-MWCNT composite were conducted in two different configurations, one is half-cell (three electrode beaker cell) and another one is full cell (CR2032 coin cell) with aqueous electrolytes. The composite electrode was prepared by mixing 80 wt% of active materials with 10 wt% Super P carbon black and 10 wt% polyvinylidene fluoride (PVDF) binder in *N*-Methyl-2-pyrrolidone (NMP) solvent. The obtained slurry coated on carbon paper and cut into 12 mm squares & 14 mm diameter circular electrodes. Mass loading for both cathode and anode materials is 1.8 and 2.7 mg/cm$^2$. In half-cell, active material coated carbon paper and large area carbon paper used as a working and counter electrodes, respectively. Standard calomel electrode (SCE) was used as a reference electrode. 10 M $NaClO_4$ aqueous electrolytes with different concentration of VC, CMC and Ag additives were used. For the full-cell tests, the $NaTi_2(PO_4)_3$-C composite on the carbon paper is used as the anode for testing Na-ion aqueous full-cells. The coin cells were assembled in an argon-filled dry glove box using a borosilicate glass-fiber separator (Whatman GF/D). The beaker half-cells were galvanostatically cycled between 0 V and 0.9 V using a potentiostat VMP3 (Biologic, France) at 1 C rate. The $NaTi_2(PO_4)_3$-C// $Na_3V_2O_{2X}(PO_4)_2F_{3-2X}$/MWCNT coin full-cells were cycled from 1 V to 1.8 V at 10 C rate based on the cathode active material weight.

## Results and Discussion

***Structural characterization.***—Fig. 1 shows the XRD patterns for the all $Na_3V_2O_{2x}(PO_4)_2F_{3-2x}$/MWCNT composites and $NaTi_2(PO_4)_3$-C along with their JCPDS data. From Fig. 1a, as-prepared $Na_3V_2O_{2x}(PO_4)_2F_{3-2x}$/MWCNT composites were matched with mixed phases of fluorophosphate and oxy- fluorophosphate.[18] Fig. 1b shows the XRD patterns for the pure NTP-C anode, which was shows high purity and crystallinity. The SEM images were presented in Fig. 2 in two different magnifications. In Figs. 2a and 2b, clearly observed that uniform distribution of MWCNT's in the $Na_3V_2O_{2x}(PO_4)_2F_{3-2x}$ sub-micron squares, which will help to increase the electronic conductivity of electrode materials. The average diagonal length of smooth edge $Na_3V_2O_{2x}(PO_4)_2F_{3-2x}$ squares with MWCNT is 2 μm. Furthermore, the carbon percentage in the composite materials was found by the Thermo Scientific Flash 2000 Series element analyzer and the value are 7.9±0.15 wt%. From Figs. 2c and 2d, the $NaTi_2(PO_4)_3$-C sample shows the highly agglomerated and the primary particle size is about 150 nm.

***Electrochemical analysis.***—Initially, we have run the charge-discharge cycles using $Na_3V_2O_{2X}(PO_4)_2F_{3-2X}$-MWCNT cathode material in aqueous electrolytes at 1 C rate (65 mA/g) with different concentration of $NaClO_4$ (1 M, 5 M & 10 M), to understand the effect of electrolytes concentrations on electrochemical performance of $Na_3V_2O_{2X}(PO_4)_2F_{3-2X}$-MWCNT in aqueous half-cell vs. carbon paper. Fig. 3 shows the cycleability data for $Na_3V_2O_{2X}(PO_4)_2F_{3-2X}$-MWCNT in aqueous half-cells with different concentrated electrolytes. From Fig. 3a, $Na_3V_2O_{2X}(PO_4)_2F_{3-2X}$-MWCNT cathode material shows the high capacity and little stable while using 10 M $NaClO_4$ electrolytes. The first discharge capacity is almost same for 1 M and 10 M, when compared to 5 M electrolytes. But, cycleability is very poor in 1 M electrolytes compared to the 5 M & 10 M electrolytes. The charge-discharge curves of $Na_3V_2O_{2X}(PO_4)_2F_{3-2X}$/MWCNT cathode material in 1 M, 5 M and 10 M electrolytes were presented in Figs. 3b, 3c and 3d, respectively. The capacity retention of $Na_3V_2O_{2X}(PO_4)_2F_{3-2X}$-MWCNT cathode material in 5 M & 10 M $NaClO_4$ solutions after 100 cycles is 83% & 68% of their initial discharge capacity values. Even though capacity retention is high in 5 M electrolytes, it has low capacity as compared

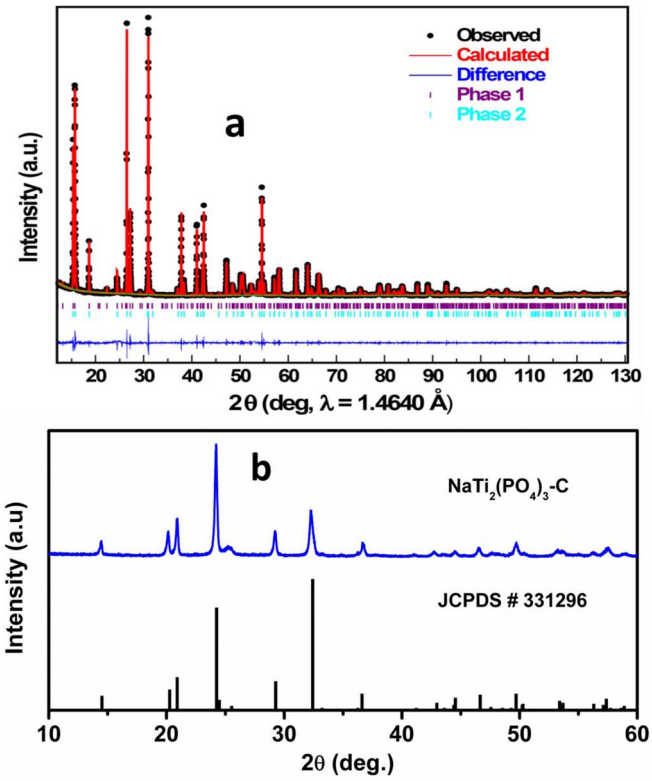


**Figure 1.** a) Synchrotron XRD patterns for the $Na_3V_2O_{2x}(PO_4)_2F_{3-2x}$-MWCNT composites and b) Powder XRD patterns for the carbon coated $NaTi_2(PO_4)_3$ with JCPDS data.

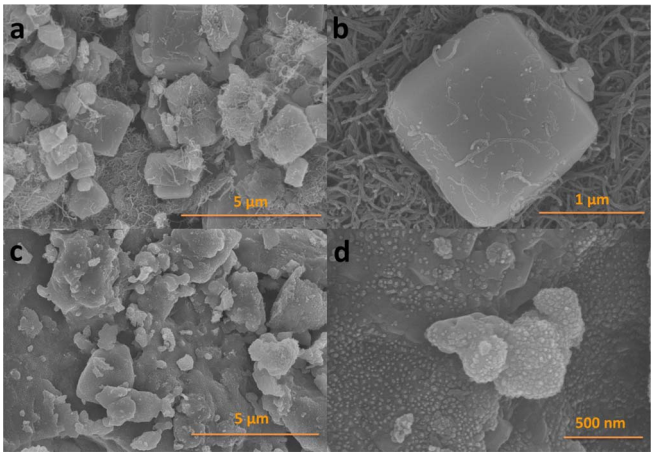


**Figure 2.** SEM images for the a, b) $Na_3V_2O_{2x}(PO_4)_2F_{3-2x}$-MWCNT composites and c, d) carbon coated NaTi2(PO4)3 in different magnifications.

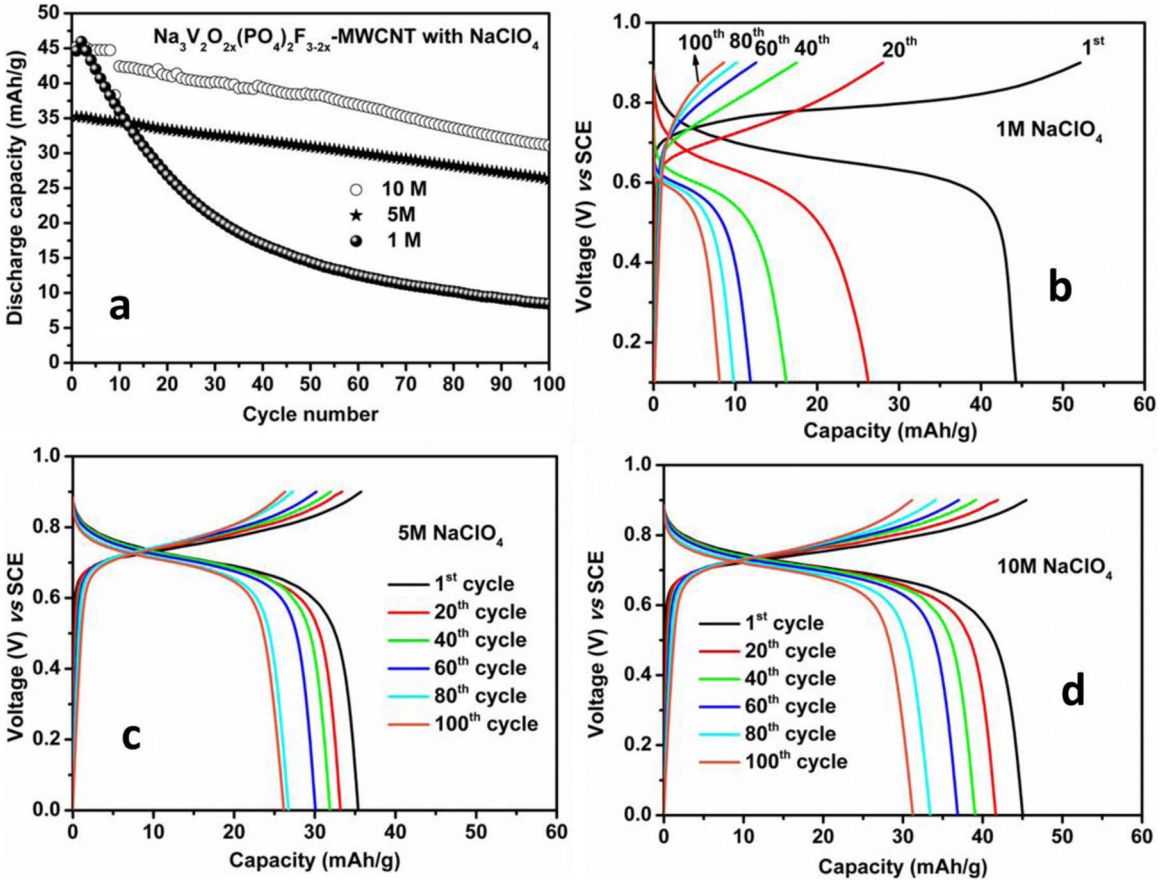


**Figure 3.** a) Cyclability of the $Na_3V_2O_{2x}(PO_4)_2F_{3-2x}$-MWCNT composites with different concentration of electrolytes. The charge –discharge curves for the b) 1 M, c) 5 M and d) 10 M $NaClO_4$ electrolytes.

to 10 M electrolytes. And also, if concentration is high of 10 M, the ionic mobility is high, obviously conductivity is also high. Furthermore, there is no other sodium based solute, which can be used for preparing 10 M concentrated aqueous electrolytes like $NaClO_4$.[20] In view of such results, we have used 10 M $NaClO_4$ electrolyte as our base electrolyte for further studies.

To increase the cyclic stability of $Na_3V_2O_{2X}(PO_4)_2F_{3-2X}$-MWCNT cathode material in 10 M $NaClO_4$ aqueous electrolyte, we have used three different additives in different concentrations based on the literature review, those are vinylene carbonate (VC), carboxymethyl cellulose (CMC) and agarose (Ag). Using gelling agents like CMC and agarose in aqueous electrolytes is not new; Mantia et al, studied the possibility to enlarge the electrochemical stability window of Li based aqueous electrolytes in previous year.[21] We have elected this same gelling agent concept to obtained stable cyclability in aqueous sodium ion batteries. Before start using these electrolytes in half cell, we have measured several physical properties of electrolytes such as hydration number, viscosity, and pH as presented in Table I. From Table I, the hydration number of Na ion in 1 M & 5 M $NaClO_4$ solutions are 16 and 6, respectively. In 10 M $NaClO_4$ solution the hydration number is four and it remains same even adding CMC and agarose. The viscosity is increasing with increasing CMC and agarose content in the solution and when compared to agarose, CMC has high viscosity values. Finally, the important parameter is pH, the pH values are quite same in all 10 M $NaClO_4$ electrolytes except 2 v% VC added solution. The 10 M $NaClO_4$ + 2 v% VC electrolytes shows highly acidic nature with pH value of 1.7. All accurate pH values are measured by using a bench top pH meter (Orion Star A221, thermo scientific). We have found the hydration number from the Raman spectra of each electrolyte. From the literature, the interaction between Na-ion and O-H groups will reflect in Raman spectra at lower wavenumber side (3100–3300 $cm^{-1}$). Hence, we have estimate the number of water molecules strongly bound to a $Na^+$ cation from intensity variation of band at 3230 $cm^{-1}$ in Raman spectrum.[22]

Fig. 4 shows the charge-discharge cycle plots for $Na_3V_2O_{2X}(PO_4)_2F_{3-2X}$-MWCNT cathode material in 10 M $NaClO_4$ aqueous with different concentration of VC as an additive. From Fig. 4a, we have used three different concentration of VC (0.5, 1 & 2 v%), among these 2 v% VC added 10 M $NaClO_4$ electrolytes shows the better performance with high stability. The $Na_3V_2O_{2X}(PO_4)_2F_{3-2X}$-MWCNT cathode material in 10 M $NaClO_4$ aqueous with 2 v% VC shows a stable capacity of 45 mAh/g at 1C

**Table I. Hydration number, Viscosity and pH values of different aqueous electrolytes.**

| Electrolyte | Hydration number | Viscosity (mPa.S) | pH |
|---|---|---|---|
| 1 M $NaClO_4$ | 16 | 2.4 | 6.9 |
| 5 M $NaClO_4$ | 6 | 3.2 | 6.4 |
| 10 M $NaClO_4$ | 4 | 4.8 | 6.0 |
| 1 M $NaClO_4$ + 2% VC | 4 | 4.9 | 1.7 |
| 1 M $NaClO_4$ + 0.25 wt% CMC | 4 | 53 | 4.3 |
| 1 M $NaClO_4$ + 0.5 wt% CMC | 4 | 96.6 | 3.9 |
| 1 M $NaClO_4$ + 0.75 wt% CMC | 4 | 326 | 4.5 |
| 1 M $NaClO_4$ + 1 wt% CMC | 4 | 501 | 4.9 |
| 1 M $NaClO_4$ + 0.25 wt% Ag | 4 | 8.1 | 4.4 |
| 1 M $NaClO_4$ + 0.5 wt% Ag | 4 | 25.4 | 4.7 |
| 1 M $NaClO_4$ + 0.75 wt% Ag | 4 | 29.4 | 4.6 |
| 1 M $NaClO_4$ + 1 wt% Ag | 4 | 45.6 | 4.5 |

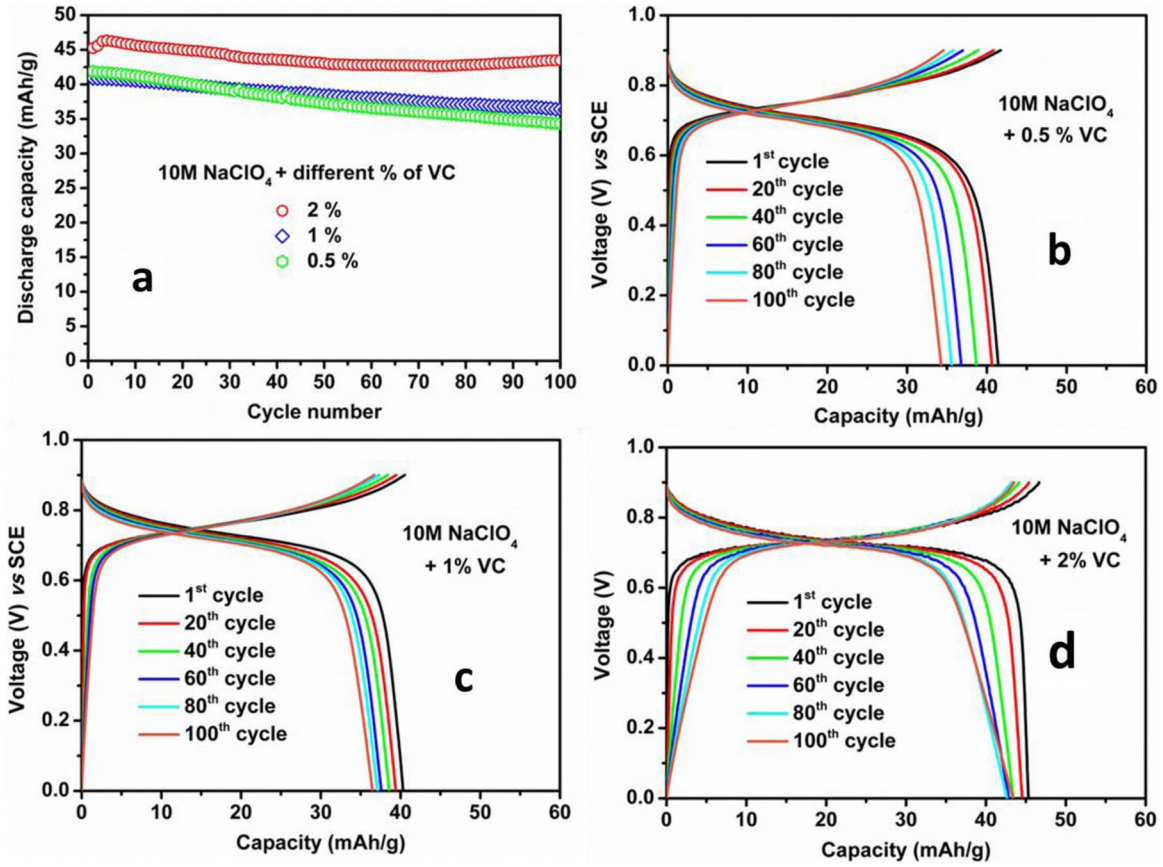


**Figure 4.** a) Cyclability of the $Na_3V_2O_{2x}(PO_4)_2F_{3-2x}$-MWCNT composites with different concentration of Vinylene carbonate (VC). The charge – discharge curves for the concentration of b) 0.5 v%, c) 1 v% and d) 2 v% VC.

(65 mA/g) and 93% of the original capacity was retained with high cycleability. It is worth to be mentioned here about the capacity difference of $Na_3V_2O_{2X}(PO_4)_2F_{3-2X}$-MWCNT cathode material in non-aqueous and aqueous electrolytes. The actual theoretical capacity of $Na_3V_2O_{2X}(PO_4)_2F_{3-2X}$ is 130 mAh/g for two Na ion intercalation and it delivers same capacity in non-aqueous electrolytes. But, in case of aqueous, only one sodium ion can be participate in intercalation/deintercalation during cycling. Hence, the theoretical capacity is decreasing to 65 mAh/g in aqueous electrolytes.[18] The charge–discharge curves of $Na_3V_2O_{2X}(PO_4)_2F_{3-2X}$-MWCNT cathode material in 10 M $NaClO_4$ with 0.5, 1, and 2 vol.% of VC are represented in Figs. 4b, 4c, and 4d, respectively. The $Na_3V_2O_{2X}(PO_4)_2F_{3-2X}$-MWCNT cathode material shows the voltage plateau at 0.73 V vs. SCE with irrespective of VC concentration in electrolytes.

Fig. 5 shows the charge-discharge cycle plots for $Na_3V_2O_{2X}(PO_4)_2F_{3-2X}$-MWCNT cathode material in 10 M $NaClO_4$ aqueous with different concentration of CMC as our second additive. In Fig. 5a, the discharge capacity versus cycle number plots for $Na_3V_2O_{2X}(PO_4)_2F_{3-2X}$-MWCNT cathode material in 10 M $NaClO_4$ with different concentration of 0.25, 0.5, 0.75 and 1 wt% of CMC were shown. The cell of 0.5 wt% CMC in 10 M $NaClO_4$ electrolytes has increased the cyclic stability of cathode material compared to other cells. From Fig. 5a, the $Na_3V_2O_{2X}(PO_4)_2F_{3-2X}$/MWCNT cathode material in 10 M $NaClO_4$ + 0.5 wt% CMC shows the first discharge capacity of 52 mAh $g^{-1}$, and 64% of the initial capacity was retained after 100 cycles at 1C rate. The charge-discharge profiles for cathode materials in 10 M $NaClO_4$ with 0.25, 0.5, 0.75, and 1 wt% are shown in Figs. 5b, 5c, 5d, and 5e, respectively. Fig. 5f shows the effect of viscosity, CMC concentration on capacity retention after 100 cycles. From Fig. 5f, both 10 M $NaClO_4$ and 10 M $NaClO_4$ + 2 vol. % VC show relatively low viscosity values like 4.8 and 4.9 mPa S, respectively. With increasing CMC concentration, the viscosity values are increasing. Capacity retention values are increasing while CMC concentration increasing from 0.25 to 0.5 wt%, and decreasing in further increasing CMC concentration to 0.75 and 1 wt%. At high viscous electrolytes (added 0.75 & 1 wt% CMC) might have constrained ionic mobility during cycling, resulting in low conductivity and stability. As we discussed before, after adding 2 vol. % of VC to 10 M $NaClO_4$ electrolytes the discharge capacity retention values are increased from 68% to 93%.

Third additive is agarose (Ag), the charge-discharge cycle plots for $Na_3V_2O_{2X}(PO_4)_2F_{3-2X}$-MWCNT cathode material in 10 M $NaClO_4$ aqueous with different concentration of agarose is shown in Fig. 6. From Fig. 6a, 10 M $NaClO_4$ electrolytes with 0.5 wt% of agarose is showing high stability compared to other percentage of additives and it shows the initial discharge capacity of 54 mAh/g and 71% of the initial capacity was retained after 100 cycles at 1 C rate. The charge-discharge profiles for cathode materials in 10 M $NaClO_4$ with 0.25, 0.5, 0.75 and 1 wt% are shown in Figs. 6b, 6c, 6d, and 6e, respectively. From Fig. 6f, agarose additive also fallowing same trend like CMC additive, but viscosity values are very low. The electrode stability (capacity retention values) is increasing by increasing viscosity up to 0.5 wt%, after words it is decreasing even increasing viscosity by adding 0.75 and 1 wt% agarose to 10 M $NaClO_4$ electrolytes.

***Effect of VC on electrochemical performance.—***After careful analyzing the effect of additives on electrochemical properties of $Na_3V_2O_{2X}(PO_4)_2F_{3-2X}$-MWCNT cathode material in aqueous electrolytes, 2 vol. % of vinylene carbonate is working as effective additive for sodium aqueous electrolytes. To understand the internal mechanism, we have discussed role of electrolyte pH and taken XPS for the

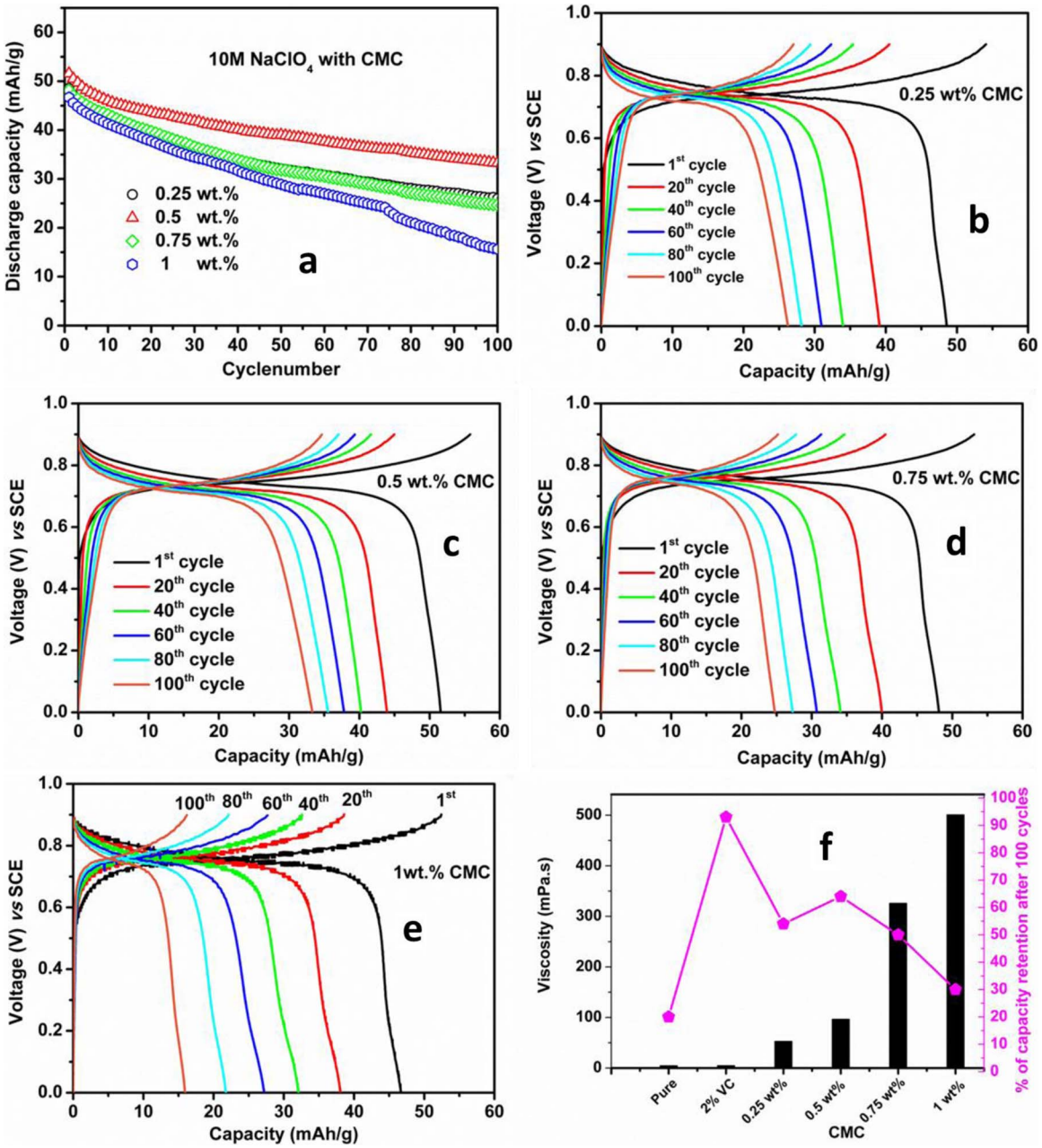


**Figure 5.** a) Cyclability of the $Na_3V_2O_{2x}(PO_4)_2F_{3-2x}$-MWCNT composites with different concentration of CMC. The charge –discharge curves for the CMC concentration of b) 0.25 wt%, c) 0.5 wt%, d) 0.75 wt%, and e) 1 wt% of CMC. f) Capacity retention versus CMC concentration plots.

$Na_3V_2O_{2X}(PO_4)_2F_{3-2X}$-MWCNT cathodes surface. Fig. 7 shows the potential versus pH plots for standard hydrogen electrode (SHE) and saturated calomel electrode (SCE) reference electrodes. From Fig. 7a, the red line black lines are represents oxygen evolution and hydrogen evolution potential limits, respectively versus SHE. The total voltage window is ~1.23 V vs. SHE. But, in this work we are using SCE as a reference electrode, the aqueous electrolyte voltage window is same like SHE, but voltage window is shifted to lower potentials, because of voltage difference between SHE and SCE (~0.244 V). The pH value of 10 M $NaClO_4$ +2 vol. % VC is 1.7, which is very low compared to all composition of electrolytes. So we draw a vertical pink dash line at pH value 1.7 in Figure 7b. The point where pink dash line intersects with red line (Oxygen evolution limit) is kind of oxygen evolution starting point for 10 M $NaClO_4$ +2 vol. % VC electrolytes. The voltage value of intersect point is 0.89 V vs. SCE. From the above discussion, it is clear that we can charge this $Na_3V_2O_{2X}(PO_4)_2F_{3-2X}$-MWCNT cathodes to 0.9 V vs. SCE very comfortably before oxygen evolution starts. Hence, the lower pH value of 10 M $NaClO_4$ +2 vol. % VC is helping to increase the aqueous battery performance and stability. And also we have avoided the corrosion reaction at these pH values by using carbon paper as our current collector. In Fig. 7b, another blue dashed line was drawn, the intersection point of this blue dashed line and red horizontal line indicate the oxygen evolution voltage for 10 M $NaClO_4$ +0.5 wt% Agarose & 10 M $NaClO_4$ +0.5 wt% CMC electrolytes (average pH value is 4.4), i.e 0.73 V. Hence, it is impossible to suppress the oxygen evolution reaction using high pH value aqueous electrolytes, while charging up to 0.9 V vs. SCE.

In literature, VC has been using as an additive for non-aqueous lithium ion batteries in the last ten years. In 2009, Prof. Gonbeau

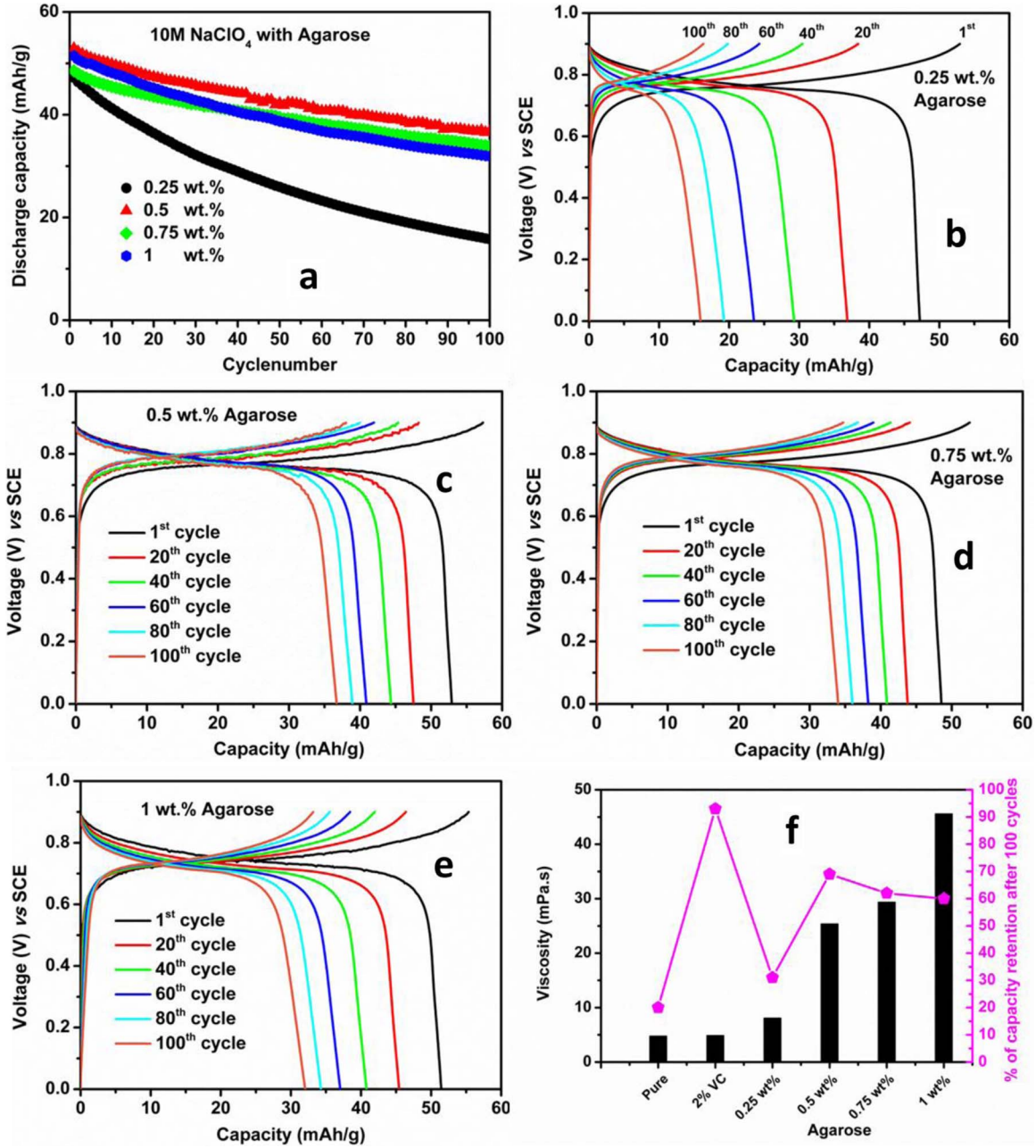


**Figure 6.** a) Cyclability of the $Na_3V_2O_{2x}(PO_4)_2F_{3-2x}$-MWCNT composites with different concentration of agarose. The charge –discharge curves for the agarose concentration of b) 0.25 wt%, c) 0.5 wt%, d) 0.75 wt%, and e) 1 wt% of agarose. f) Capacity retention versus agarose concentration plots.

and prof. Dahn research groups have done enough investigation on effect of VC in $LiCoO_2$, $LiFePO_4$/C, and $LiCoO_2/Li_4Ti_5O_{12}$ electrode materials in non-aqueous Li-ion batteries.[23–25] And they concluded that formation of passivation films at the surface of the electrodes, which consists of degradation products of VC. Prof. Mentus group demonstrated effect of VC on $Li_{1.05}Cr_{0.10}Mn_{1.85}O_4$ electrode material in a saturated $LiNO_3$ aqueous solution.[26] In present work, we have investigated the effect of VC on electrochemical properties of $Na_3V_2O_{2X}(PO_4)_2F_{3-2X}$/MWCNT cathodes in sodium aqueous electrolytes by XPS analysis for electrodes surface. Figs. 8a and 8b, shows the C 1s core peaks of the both as prepared and fully charged electrode in 2 vol. % VC added 10 M $NaClO_4$ aqueous electrolytes. From Fig. 8a, the spectra are deconvoluted into four Gaussian peaks centered at 284.4, 285.3, 287.5, and 291.0 eV. Here, the main peak at 284.4 eV originates from a graphite signal. The peak at 285.3 eV is attributed to $sp^3$ carbon.[27,28] The peaks at 287.5, and 291.0 eV correspond to carbonyl (or ether), and carboxyl (or ester) groups, respectively, which is close to PVDF signatures. In Fig. 8b, all peak intensities are decreasing except peak at 287.5 (C=O). The intensity of this peak is greater in 2% VC added electrolytes, which exposure a specific reactivity of this electrolyte against the electrode surface. Figs. 8c and 8d, shows the O 1s core peaks of the both as prepared and fully charged electrode in 2 vol. % VC added 10 M $NaClO_4$ aqueous electrolytes. From Fig. 8c, the peak at 530.6, 532.4 and 535.5 eV are belongs to the V-O, oxygen atoms of $PO_4^{3-}$ phosphate groups and O-$F_x$ components. In Fig. 8d, along with above signature O 1s peak of $Na_3V_2O_{2X}(PO_4)_2F_{3-2X}$/MWCNT, the fully charged sample in 2 vol. % VC added 10 M $NaClO_4$ aqueous electrolytes shows the new high intensity peak at 533.3 eV, which belongs to the C=O. In both cases (Carbon and Oxygen XPS results), the significant peak of C=O become strong in 2% VC added electrolytes, which indicates the formation of passivation layer, composites with degradation products of

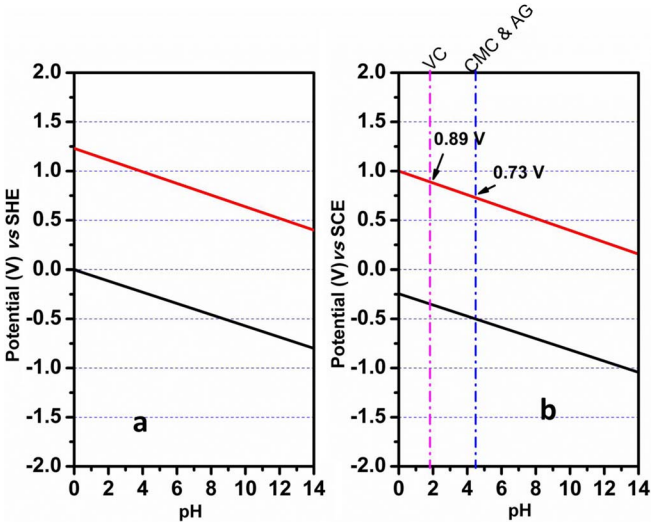


**Figure 7.** Electrochemical stability voltage window for the reference electrode of a) Standard hydrogen electrode (SHE) and b) Saturated calomel electrode (SCE), the pink vertical dashed line indicates the pH values of 2 v% VC added 10 M $NaClO_4$ electrolytes and blue vertical dashed line indicates the pH values of 0.5 wt% of agarose & 0.5 wt% of CMC added 10 M $NaClO_4$ electrolytes.

VC. Hence, using 2 vol. % of VC is more efficient in terms of high voltage and stable cyclability by decreasing pH values below 2 and formation of passivation layer on electrode surfaces.

***Full cell with $NaTi_2(PO_4)_3$-C.***—After half-cell fabrication, we have also prepared full cell with selected electrolyte compositions by using anode material [$NaTi_2(PO_4)_3$-C] in CR2032 coin cells. Discharge capacity versus cycle number plots for $NaTi_2(PO_4)_3$-C// $Na_3V_2O_{2X}(PO_4)_2F_{3-2X}$-MWCNT full cell with using additives 2 vol. % VC, 0.5 wt% CMC, 0.5 wt% Ag and 2 vol. % VC + 0.5 wt% Ag in 10 M $NaClO_4$ aqueous electrolytes. From the Fig. 9a, $NaTi_2(PO_4)_3$-C// $Na_3V_2O_{2X}(PO_4)_2F_{3-2X}$-MWCNT full cell delivers first discharge capacity of 39 mAh $g^{-1}$ at 10 C (650 mA $g^{-1}$), after few cycles, it was stabilized at 35 mAh $g^{-1}$ in 10 M $NaClO_4$ + 2 vol. % VC aqueous electrolytes. In case of using 10 M $NaClO_4$ with both 2 vol. % VC and 0.5 wt% Ag as aqueous electrolytes, the $NaTi_2(PO_4)_3$-C// $Na_3V_2O_{2X}(PO_4)_2F_{3-2X}$-MWCNT full cell delivered a stable capacity of 30 mAh $g^{-1}$. $NaTi_2(PO_4)_3$-C// $Na_3V_2O_{2X}(PO_4)_2F_{3-2X}$-MWCNT full cell in 0.5 wt% CMC and 0.5 wt% Ag in 10 M $NaClO_4$ aqueous electrolytes shows less stability compared to others. The charge-discharge curves of $NaTi_2(PO_4)_3$-C// $Na_3V_2O_{2X}(PO_4)_2F_{3-2X}$-MWCNT full cell with 2 vol. % VC, 0.5 wt% CMC, 0.5 wt% Ag, and 2 vol.% VC + 0.5 wt% Ag in 10 M $NaClO_4$ aqueous electrolytes are presented in Figs. 9b, 9c, 9d, and 9e, respectively. Fig. 9f shows the cyclic voltammetry for $NaTi_2(PO_4)_3$-C in half-cell configuration and it shows highly stable CV plots up to 60 cycles at scanning rate of 0.5 mV/s in 10 M $NaClO_4$ + 2 v% VC electrolytes. All cells showed the voltage plateau at ~1.5 V, and with compared to the half-cells, the full cells were more stable because of using sealed coin cells and very low electrolyte contents, which can reduce the influence of oxygen. By adding VC to 10 M $NaClO_4$ electrolytes, we can utilize aqueous high voltage window through reducing the pH values and it will form a passivation film on electrode surface that can be responsible for stable cycleability. Finally, using vinylene carbonate as an additive in

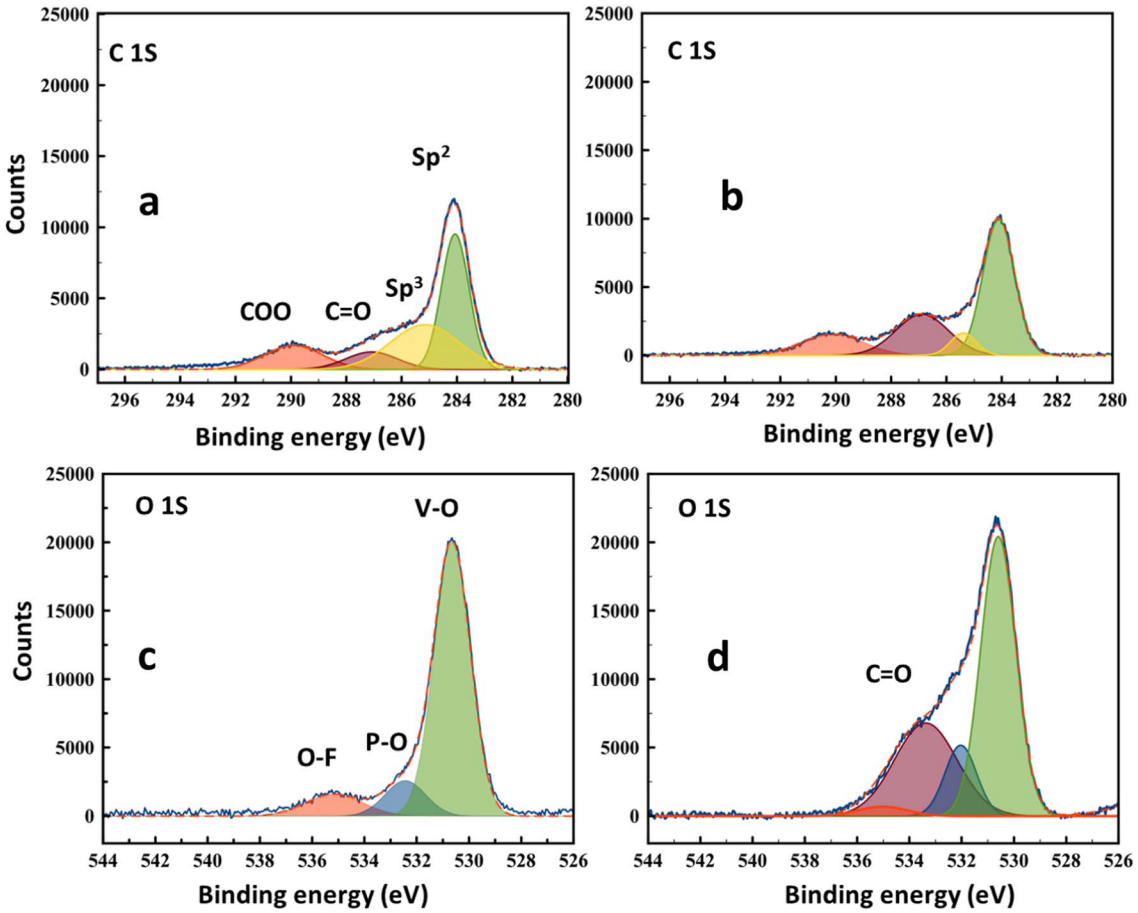


**Figure 8.** a, c) the carbon and oxygen XPS spectra of as prepared $Na_3V_2O_{2x}(PO_4)_2F_{3-2x}$-MWCNT composites electrode and b, d) the carbon and oxygen XPS spectra of fully charged $Na_3V_2O_{2x}(PO_4)_2F_{3-2x}$-MWCNT composites electrode.

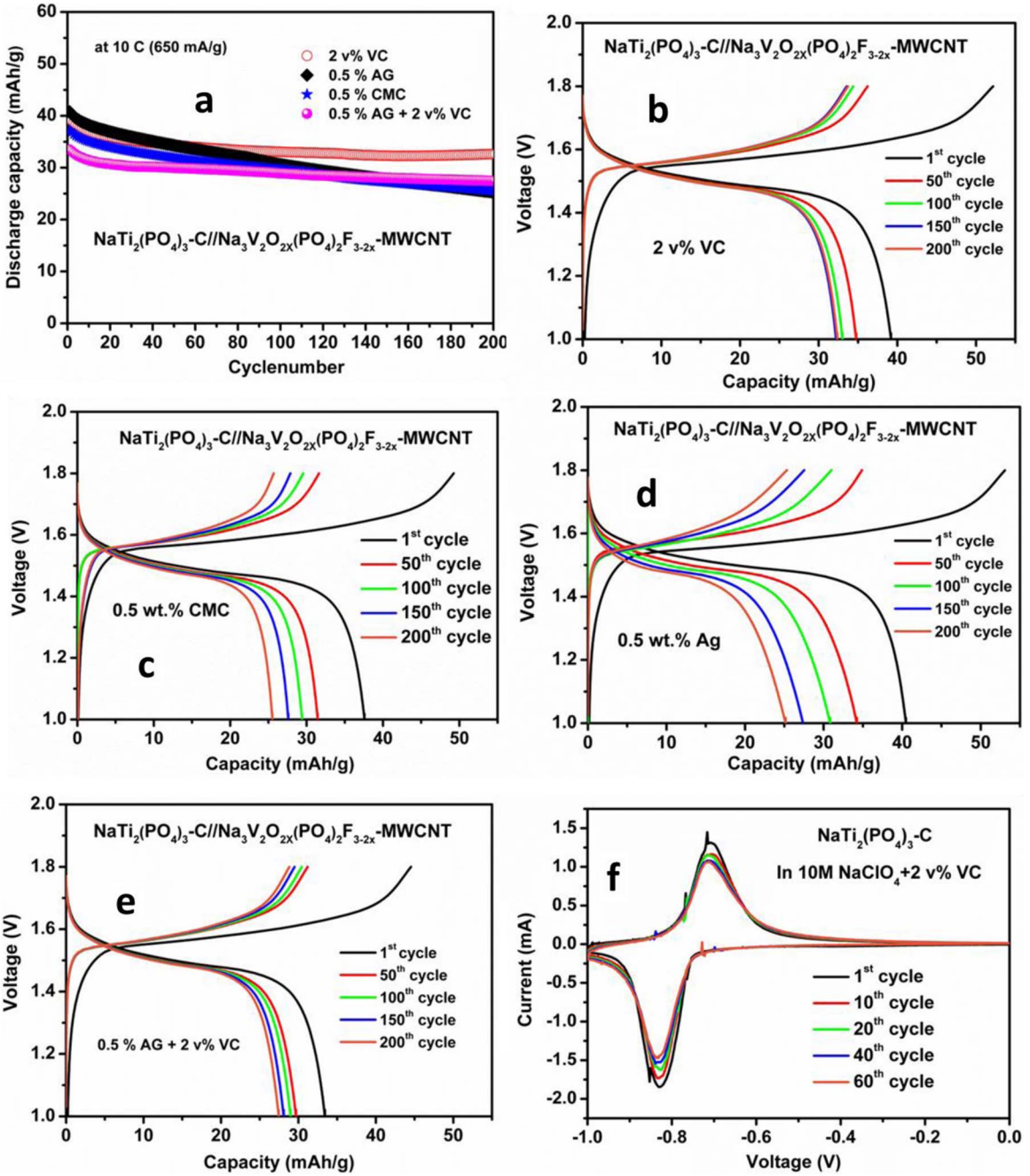


**Figure 9.** a) Cyclability of the $NaTi_2(PO_4)_3$-C// $Na_3V_2O_{2x}(PO_4)_2F_{3-2x}$-MWCNT aqueous full cells with different combination of additives. The charge –discharge curves for b) 2 v% of VC c) 0.5 wt% of agarose, d) 0.5 wt% of CMC, and e) 0.5 wt% of agarose + 2 v% of VC. f) CV plots for the $NaTi_2(PO_4)_3$-C in 10 M $NaClO_4$ + 2 v% VC aqueous electrolytes.

sodium based aqueous electrolytes is a beneficial for low cost aqueous rechargeable sodium ion batteries.

## Conclusions

The effect of electrolytes concentration and additives (VC, CMC & Agarose) on the electrochemical performance and stability of $NaTi_2(PO_4)_3$-C// $Na_3V_2O_{2X}(PO_4)_2F_{3-2X}$-MWCNT aqueous sodium ion battery system was investigated using charge-discharge cycling. From the analysis,

1. The cycleability of $Na_3V_2O_{2X}(PO_4)_2F_{3-2X}$/MWCNT cathode with 10 M $NaClO_4$ aqueous electrolytes is increased, which is due to the high ionic mobility and low dissolved oxygen content.
2. Adding 2 vol. % of VC in 10 M $NaClO_4$ aqueous electrolytes, the performance and stability of $Na_3V_2O_{2X}(PO_4)_2F_{3-2X}$/MWCNT half-cell is enhanced significantly. The reason behind is that, the pH value of 2 vol. % of VC added 10 M $NaClO_4$ aqueous electrolytes is 1.7, at this low pH values the cell can be cycled comfortably between 0 ~ 0.9 V vs. SCE. Furthermore, the XPS results support the evidence of passivation layers on electrode surface, resulting in high cyclic stability of electrode materials.
3. Furthermore, there is no corrosion like side reactions even at high concentrated electrolytes with low pH values while using carbon paper as a current collector.
4. Altogether, $NaTi_2(PO_4)_3$-C//$Na_3V_2O_{2X}(PO_4)_2F_{3-2X}$/MWCNT full cell delivers stable discharge capacity of 35 mAh/g at 10 C.

The effect of low cost acetic additives on stability and broadening of voltage window to obtain full capacity from cathode material issues will be a topic of future work.

## Acknowledgments

This work was supported by the Program to Solve Climate Changes (NRF-2010-C1AAA001-2010-0029031) of Korea (NRF) funded by the Ministry of Science, ICT & Future Planning. The authors acknowledge technical support from staffs of the 9B-HRPD beamline at Pohang Accelerator Laboratory (PAL) in the experiments.

## References

1. Y. Wu, *Lithium-ion batteries*, CRC press, New York (2015).
2. P. Moseley, J. Garche, and P. Adelmann, *Electrochemical energy storage for renewable sources and grid balancing*, Elsevier, USA (2015).
3. P. Balakrishnan, R. Ramesh, and T. Prem Kumar, *J. Power Sources*, **155**, 401 (2006).
4. Q. Wang, P. Ping, X. Zhao, G. Chu, J. Sun, and C. Chen, *J. Power Sources*, **208**, 210 (2012).
5. H. Kim, J. Hong, K. Park, H. Kim, S. Kim, and K. Kang, *Chem. Rev.*, **114**, 11788 (2014).
6. Y. Wang, J. Yi, and Y. Xia, *Adv. Energy Mater.*, **2**, 830 (2012).
7. W. Li, J. Dahn, and D. Wainwright, *Science*, **264**, 1115 (1994).
8. R. Ruffo, C. Wessells, R. Huggins, and Y. Cui, *Electrochem. Commun.*, **11**, 247 (2009).
9. H. Yadegari, A. Jabbari, and H. Heli, *J Solid State Electrochem.*, **16**, 227 (2011).
10. H. Wang, K. Huang, Y. Zeng, S. Yang, and L. Chen, *Electrochim. Acta*, **52**, 3280 (2007).
11. G. Wang, N. Zhao, L. Yang, Y. Wu, H. Wu, and R. Holze, *Electrochim. Acta*, **52**, 4911 (2007).
12. J. Luo, W. Cui, P. He, and Y. Xia, *Nat. Chem.*, **2**, 760 (2010).
13. Z. Li, D. RavnsbÃ ¦ k, K. Xiang, and Y. Chiang, *Electrochem. Commun.*, **44**, 78 (2014).
14. Z. Li, D. Young, K. Xiang, W. Carter, and Y. Chiang, *Adv. Energy Mater.*, **3**, 290 (2012).
15. X. Wu, Y. Cao, X. Ai, J. Qian, and H. Yang, *Electrochem. Commun.*, **31**, 145 (2013).
16. B. Zhang, Y. Liu, X. Wu, Y. Yang, Z. Chang, Z. Wen, and Y. Wu, *Chem. Commun.*, **50**, 1209 (2014).
17. X. Wu, M. Sun, Y. Shen, J. Qian, Y. Cao, X. Ai, and H. Yang, *ChemSusChem*, **7**, 407 (2014).
18. P. R. Kumar, Y. Jung, C. Lim, and D. Kim, *J. Mater. Chem. A*, **3**, 6271 (2015).
19. M. VujkoviÄ, M. MitriÄ, and S. Mentus, *J. Power Sources*, **288**, 176 (2015).
20. W. Wu, S. Shabhag, J. Chang, A. Rutt, and J. Whitacre, *J. Electrochem. Soc.*, **162**, A803 (2015).
21. J. StojadinoviÄ, A. Dushina, R. TrÃcoli, and F. La Mantia, *ChemPlusChem*, **79**, 1507 (2014).
22. J. Yin, C. Zheng, L. Qi, and H. Wang, *J. Power Sources*, **196**, 4080 (2011).
23. L. El Ouatani, R. Dedryvère, C. Siret, P. Biensan, S. Reynaud, P. Iratçabal, and D. Gonbeau, *J. Electrochem. Soc.*, **156**, A103 (2009).
24. L. El Ouatani, R. DedryveÌre, C. Siret, P. Biensan, and D. Gonbeau, *J. Electrochem. Soc.*, **156**, A468 (2009).
25. D. Xiong, J. Burns, A. Smith, N. Sinha, and J. Dahn, *J. Electrochem. Soc.*, **158**, A1431 (2011).
26. I. Stojković, N. Cvjetićanin, and S. Mentus, *Electrochem. Commun.*, **12**, 371 (2010).
27. A. Felten, C. Bittencourt, J. Pireaux, G. Van Lier, and J. Charlier, *J. Appl. Phys.*, **98**, 074308 (2005).
28. H. Ago, T. Kugler, F. Cacialli, W. Salaneck, M. Shaffer, A. Windle, and R. Friend, *J. Phys. Chem. B*, **103**, 8116 (1999).